Pediatric RESEARCH

BASIC SCIENCE ARTICLE

Caspase-1 involves in bilirubin-induced injury of cultured rat cortical neurons

Chunmei He[1,2,3], Jie Feng[1], Hongmei Huang[1,3] and Ziyu Hua[1,2]

BACKGROUND: Bilirubin encephalopathy, the most serious complication of hyperbilirubinemia during the neonatal period, with high mortality and morbidity, often causes irreversible neurological damage. Currently, caspase-1, a member of the cysteinyl aspartate-specific protease caspase family, is regarded as a key mediator of inflammatory processes, attracting widespread attention. The purpose of this study was to investigate whether caspase-1 is involved in bilirubin-induced neuronal injury.
METHODS: VX-765, a highly potent and selective inhibitor of caspase-1, was used to investigate the effects of unconjugated bilirubin (UCB) on rat cortical neurons, including cell viability, morphological changes in the cell membrane, and nuclear factor-kappa B (NF-κB) activation.
RESULTS: Neurons treated with UCB showed increased caspase-1 activity without the secretion of interleukin (IL)-1β and IL-18, and caspase-1 was significantly inhibited by pretreatment with VX-765. The cell viability of the VX-765-pretreated neurons was improved, and cell membrane rupture was prevented, as detected by lactate dehydrogenase release and ethidium bromide uptake. Moreover, NF-κB activation by UCB exposure, was attenuated by VX-765 pretreatment.
CONCLUSION: Bilirubin-induced neuronal injury involves the activation of caspase-1 and NF-κB, leading to membrane leakage, independently of IL-1β and IL-18.

Pediatric Research (2019) 86:492–499; https://doi.org/10.1038/s41390-019-0451-3

INTRODUCTION

Hyperbilirubinemia remains one of the most frequent clinical phenomena among neonates. Approximately 85% of full-term infants and most premature infants have transient hyperbilirubinemia during newborn phase.[1,2] Bilirubin encephalopathy is the most serious complication of hyperbilirubinemia during neonatal period, with high mortality and morbidity. Some patients survive with the sequelae of central nervous system, such as bradykinesia and hearing impairment,[3,4] reflecting the regions of central nervous system vulnerable to bilirubin neurotoxicity, including the basal ganglia, especially the globus pallidus, substantia nigra, and auditory brainstem.[1] Currently, bilirubin encephalopathy continues to be reported worldwide as a problem with wide regional and national variation.[5] The detailed identification of the neurological events and molecular targets triggering bilirubin neurotoxicity will help with the understanding and management of this disease.

In recent years, studies have shown that bilirubin neurotoxicity is associated with mitochondrial dysfunction, oxidative stress, excitotoxicity, and myelin damage, eventually leading to apoptosis and the necrosis of nerve cells, accompanied by the inflammation infiltration of the nervous system.[6,7] The inflammatory response is a complicated cascade process related to an organism's defense against infection and damage. Some recent studies have suggested an important role of the inflammatory response in the occurrence and development of noninfectious neurological diseases, such as Parkinson's disease and ischemic stroke.[8,9] In the study of bilirubin encephalopathy, inflammation plays a similar role.[10] Our previous experiments detected the release of inflammatory cytokines in both animal and cell models of bilirubin encephalopathy, whereas the inhibition of the process reduced cell death and alleviated bilirubin neurotoxicity.[11,12] Therefore, it is worth investigating the correlation between inflammation and bilirubin neurotoxicity.

Caspase-1, a member of the cysteinyl aspartate-specific protease caspase family, requires the assembly of multiprotein complexes known as inflammasomes for proteolytic activation.[13] In recent years, caspase-1 has been regarded as a key mediator of inflammatory processes, cleaving and processing the proinflammatory cytokines interleukin (IL)-1β and IL-18, ultimately causing a highly inflammatory form of programmed cell death.[14] Our previous experiments showed that caspase-1 is involved in unconjugated bilirubin (UCB)-induced astrocyte damage.[15] VX-765, a highly potent and selective inhibitor of caspase-1, has been used in the therapy of chronic epilepsy and psoriasis, and it has been proven to be safe and well tolerated during a 6-week phase IIa trial in patients with treatment-resistant partial epilepsy.[16,17] VX-765 showed a protective effect against astrocytes induced by UCB[15] and consequently improved the neurological outcome of kernicterus model rats (an unpublished study). Traditionally, neurons are considered the most important cells in the central nervous system, regulating the development of the brain. Does VX-765 have a similar effect on neurons? According to the preliminary experiment, VX-765 improved the survival rate of UCB-treated neurons. Therefore, the purpose of the study is to investigate whether caspase-1 is involved in bilirubin cytotoxicity in neurons.

[1]Department of Neonatology, Children's Hospital of Chongqing Medical University, Ministry of Education Key Laboratory of Child Development and Disorders, 400014 Chongqing, China; [2]China International Science and Technology Cooperation base of Child development and Critical Disorders, 400014 Chongqing, China and [3]Chongqing Key Laboratory of Child Infection and Immunity, 400014 Chongqing, China
Correspondence: Ziyu Hua (h_ziyu@126.com)

Received: 28 January 2019 Revised: 24 May 2019 Accepted: 29 May 2019
Published online: 13 June 2019

METHODS

Reagents

Bilirubin (B4126), ethidium bromide (EtBr) (E1385), and 3-(4,5-dimethyl-2-thiazolyl)-2,5-diphenyl-2-H-tetrazolium bromide (MTT) (M5655) were purchased from Sigma-Aldrich, Co. (St. Louis, MO). Ethidium homodimer-2 (EthD2) (E3599) was purchased from Life Technologies (Eugene, OR). VX-765 (S2228) was purchased from Selleck Chemicals (Houston, TX). The Caspase-Glo 1 assay was purchased from Promega (Madison, WI). Anti-Gasdermin D (anti-GSDMD) antibody (93709), anti-nuclear factor-kappa B (NF-κB) p65 antibody (8242), anti-Histone H3 antibody (4499), and anti-β-actin (3700) were purchased from Cell Signaling Technology (Danvers, MA). Anti-NeuN antibody (ab177487) was purchased from Abcam (Cambridge, UK). The nonradioactive infrared NF-κB electrophoretic mobility shift assay (EMSA) Kit was purchased from Viagen Biotech (Changzhou, China). The enzyme-linked immunosorbent assay (ELISA) kits for IL-1β, IL-18, IL-6, and tumor necrosis factor (TNF)-α were purchased from Raybiotech (Norcross, GA). QuantiNova SYBR Green PCR Kit (208054) was purchased from Qiagen (Hilden, Germany).

Cell culture

Neurons were isolated from the cerebral cortices of the 17–19-day-old fetuses of pregnant Sprague Dawley rats, as previously described,[18] with minor modifications. In short, the fetuses were rapidly decapitated. After the removal of the meninges, blood vessels, and white matter, the cerebral cortex was cut into small pieces in cold Dulbecco's Modified Eagle Medium (DMEM). The pieces were treated with 0.25% trypsin for 20 min at 37 °C. After neutralizing the trypsin in DMEM containing 10% fetal bovine serum, the cells were resuspended in DMEM and plated on culture dishes or 24-/96-well plates precoated with poly-D-lysine at a density of 2.0×10^5 cells/cm^2. The cultures were maintained in a humidified atmosphere of 5% CO_2 at 37 °C. After 4–6 h, the media were changed to Neurobasal media supplemented with 0.5 mM L-glutamine, 2% B-27 supplement, and penicillin–streptomycin. Every 3 days, half of the old medium in each cell was removed and replaced by the same volume of fresh medium.

Bilirubin solution preparation and cell treatment

Bilirubin was dissolved in dimethyl sulfoxide (DMSO) solution (17.1 mM), and HCl was used to restore the pH value to 7.4. The bilirubin solution was stored at −20 °C, protected from light. VX-765 was dissolved in DMSO solution (50 mM) and stored at −80 °C. The neurons were cultured for 8 days in vitro and were randomly divided into three groups: the control group, the UCB group, and the VX-765 + UCB group. The neurons in the UCB group were incubated with 50 μM UCB in the presence of 100 μM human serum albumin (HSA) (UCB/HSA molar ratio of 0.5).[19] The neurons in the VX-765 + UCB group were pretreated with 50 μM VX-765 for 1 h before incubating with the same concentration of UCB and HSA. In addition, the neurons in the control group were incubated with equal volumes of DMSO and HSA.

Immunocytochemistry assay

Neurons were cultured on coverslips in 24-well plates. The cells were fixed with 4 % paraformaldehyde, treated with 0.1% Triton and blocked with 2% bovine serum albumin, incubated overnight at 4 °C with a anti-NeuN antibody (1:200), and then incubated with fluorescence secondary antibody for 1 h at room temperature, next stained with DAPI. Coverslips were analyzed using a fluorescence microscope (Nikon, Japan).

Modified MTT assay

The modified MTT method was used to detect the survival of neurons cultured on 96-well plates.[20] The cells were grouped and stimulated by bilirubin at the corresponding time point. The cells were incubated with the MTT (5 mg/ml, 20 μl/well), protected from light, for 4 h at 37 °C. Then the medium was carefully discarded, and the MTT formazan crystals were dissolved in isopropanol/HCl (0.04 M, 160 μl/well) for 15 min with gentle shaking at room temperature. The supernatant containing the dissolved MTT formazan was carefully transferred into another clean 96-well plate to measure the optical density of each well at 570 nm.

Lactate dehydrogenase (LDH) release assay

LDH in the culture supernatant of neurons was detected to assess the extent of cell membrane damage. The LDH cytotoxicity detection kit (Beyotime) was used as directed by the manufacturer. The cells of the positive control group were treated with LDH release reagent and were allowed the outflow of LDH. The absorbance of each well was detected at 490 nm by a microplate reader (Synergy H1266849, Wilmington, DE), and the results are expressed as a percentage of LDH release.

Caspase-1 activity assay

The caspase-1 assay was based on the ability of caspase-1 to act on Z-WEHD-aminoluciferin and generate light by recombinant luciferase. According to the manufacturer's instructions, neurons were cultured in multiwell plates that were compatible with the luminometer (Synergy H1266849, Wilmington, DE). The cells were incubated with the prepared working reagents at room temperature. The luminescence of each well was measured by a luminometer, as directed by the luminometer manufacturer. The cells generated a luminescent signal, which was proportional to the caspase-1 activity.

EtBr and EthD2 staining

Two red membrane-impermeant dyes, EtBr (molecular weight (MW) 394 Da) and EthD2 (MW 1293 Da), were used to investigate the membrane pore formation of neurons.[21] Neurons were cultured on coverslips in 24-well plates. The cells of the positive control group were treated with 0.1% Triton X-100 and uniformly allowed the influx of both EtBr and EthD2. At the corresponding time point, the cells of each group were stained with either EtBr (25 μg/ml) or EthD2 (25 μg/ml) and counterstained with the Hoechst 33342, a blue membrane-permeable dye to mark cell nucleus. A cell positively stained with two dyes is regarded as a positive cell. Coverslips were analyzed using a fluorescence microscope.

Quantitative real-time PCR

The total RNA was isolated (Bioteke) and synthesized into cDNA (TaKaRa). Relative mRNA levels were determined using the Bio-Rad iCycler and SYBR Green method. Reverse transcriptase-PCR was performed with glyceraldehyde-3-phosphate dehydrogenase (GAPDH) as the internal reference gene. Primer pairs: IL-1β (Forward: TCCTTGTGCAAGTGTCTGAAGC, Reverse: TCATCTGGACA GCCCAAGTCA), IL-18 (Forward: ACAACCGCAGTAATACGGAGC, Reverse: GGATTCGTTGGCTGTTCGGT), and GAPDH (Forward: AGTGCCAGCCTCGTCTCATA, Reverse: AAGAGAAGGCAGCCCTGGT AA). PCR Ct values were obtained to calculate mRNA relative expression. Values are expressed as the fold increase in the mRNA levels of the control group.

Enzyme-linked immunosorbent assay

The protein levels of IL-1β, IL-18, IL-6, and TNF-α from the cultured supernatant of neurons were measured by ELISA kits according to the manufacturer's directions. The absorbance of the samples was detected at 450 nm by a microplate reader. All samples were tested in duplicate.

Western blot analysis

The nuclear proteins (Viagen) were prepared to measure the protein level of NF-κB, while total proteins were extracted for GSDMD. The proteins separated by 12% sodium dodecyl sulfate-polyacrylamide

gel electrophoresis and transferred to polyvinylidene difluoride membranes. The membranes were blocked with 5% nonfat milk for 1 h at room temperature, incubated overnight at 4 °C with a primary antibody (anti-NF-κB p65 1:1000, anti-Histone H3 1:2000, anti-GSDMD 1:1000, or anti-β-actin 1:5000), and then incubated with an horseradish peroxidase-conjugated anti-rabbit secondary antibody (1:2000) for 1 h at room temperature. The protein bands were visualized with a G-BOX imaging system (Syngene, Cambridge, UK) using an ECL Assay Kit (Bio-Rad, Hercules, CA).

Electrophoretic mobility shift assays

The nuclear proteins were prepared. According to the instructions of nonradioactive infrared NF-κB EMSA kit, the mixture was prepared and incubated with an IR700-labeled oligonucleotide bio-NF-κB probe (5′-AGTTGAGGGGACTTTCCCAGGC- 3′), then subjected to 5% nondenatured polyacrylamide gel electrophoresis. The gels were visualized using an Odyssey fluorescence detector (Li-Cor, Lincoln, NE).

Statistical analysis

The statistical analyses were performed with SPSS (version 17.0). The data are presented as the means and SDs. Initially, a normality test and a homogeneity test for variance were performed. If the data were in compliance with a normal distribution and showed homogeneity of variance, analysis of variance with Bonferroni's post-test or Student's *t*-test was performed; otherwise, a rank-sum test was used. Categorical data were analyzed using the chi-squared test. $p < 0.05$ was considered statistically significant.

RESULTS

Immunocytochemistry and morphology methods were employed to evaluate the purity of neuronal cultures (Fig. 1a–e). The percentage of NeuN-positive cells was >95%, so primary cultured cortical neurons were eligible for the following experiments.

VX-765 decreased bilirubin-induced neuronal death

A modified MTT assay was employed to analyze whether UCB induced the loss of cell viability in neurons. The results showed that cell viability decreased with the time of UCB stimulation. The relative survival rate of cells with UCB at 24 h was 40.230 ± 2.614% ($p < 0.001$, Fig. 1f). Based on the pharmacological features, VX-765 was administered 1 h before UCB stimulation. The survival rate of each group stimulated with UCB for 24 h was measured. The relative survival rate of the VX-765 + UCB group was 73.029 ± 5.681%, which was significantly higher than that of the UCB group ($p < 0.001$, Fig. 1g) and lower than that of the control group ($p < 0.001$, Fig. 1g).

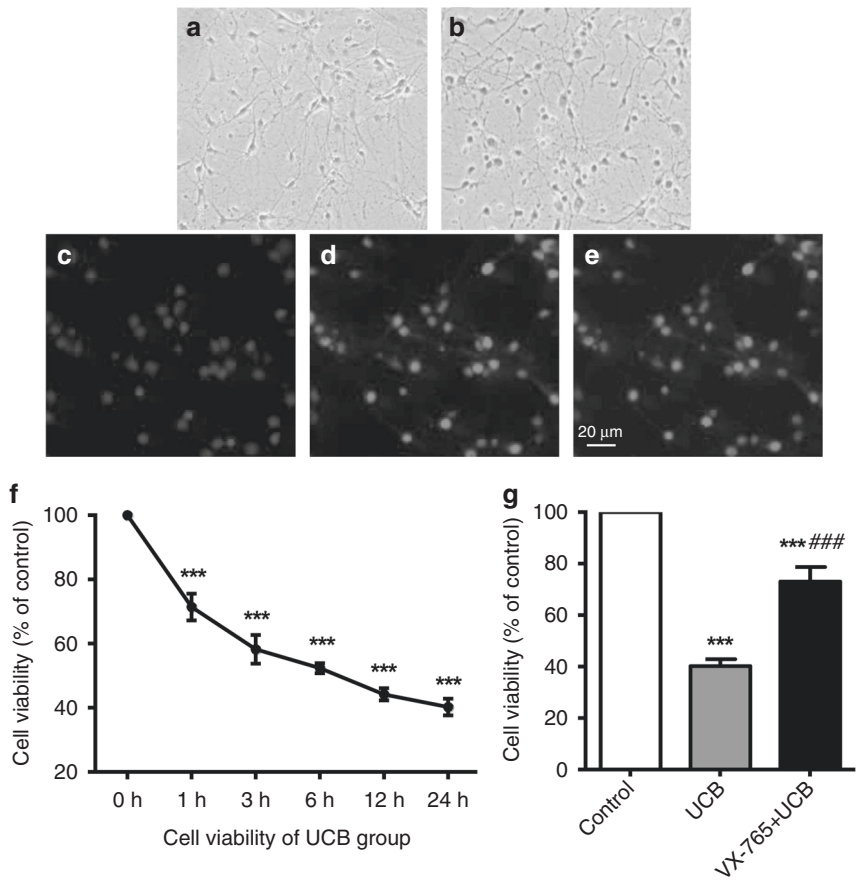

Fig. 1 Effects of VX-765 and unconjugated bilirubin (UCB) on cell viability. **a** The cortical neurons were cultured for 8 days in vitro. **b** The cortical neurons were treatment with 50 μM UCB. Immunocytochemical method was used to detect the purity of neuronal cultures using neuronal marker NeuN (**c** DAPI, **d** NeuN, **e** Merge). The adherent cells were visualized by inverted microscope and fluorescence microscopy (×20 objective). **f** Cell viability was detected with the modified MTT (3-(4,5-dimethyl-2-thiazolyl)-2,5-diphenyl-2-H-tetrazolium bromide) assay, presented as a percentage of the control. Cell viability decreased in a time-dependent manner after treatment with UCB. ***$p < 0.001$, versus the control group (0 h) using the chi-squared test. **g** The cells in each group were treated for 24 h as previously described. ***$p < 0.001$, versus the control group; $^{###}p < 0.001$, versus the UCB group using the chi-squared test. Three independent experiments were performed in duplicate. Error bar, SD

VX-765 suppressed bilirubin-induced caspase-1 activation

Subsequently, we investigated whether UCB activated caspase-1 in neurons. The results showed that the level of caspase-1 activation was markedly increased at 3, 6, and 12 h compared with those of the control groups at the corresponding time points (all p values < 0.001, Fig. 2), whereas the level of caspase-1 activation at 24 h had decreased to a level similar to that seen at 1 h. Next, the effect of VX-765 on the UCB-induced activation of caspase-1 in neurons was observed. The caspase-1 activities in the VX-765+UCB groups at 3, 6, and 12 h were significantly inhibited compared to those of the UCB groups at the corresponding time points (all p values < 0.001, Fig. 2); meanwhile, there was no significant difference compared with the control groups ($p > 0.05$, Fig. 2).

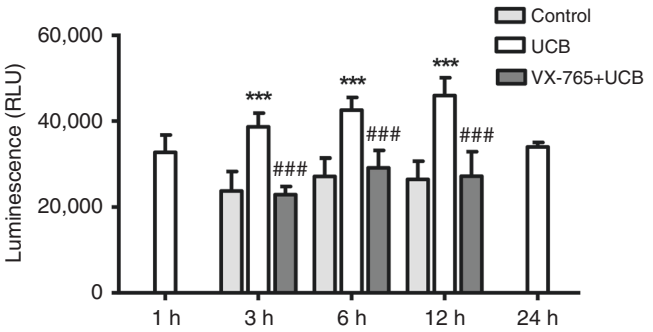

Fig. 2 Unconjugated bilirubin (UCB)-induced caspase-1 activation in cultured rat cortical neurons. Caspase-1 activity was measured at the corresponding time points after UCB treatment. The levels of caspase-1 activation were attenuated with VX-765 pretreatment at 3, 6, and 12 h. $^{***}p < 0.001$, versus the control group at the corresponding time points; $^{###}p < 0.001$, versus the UCB group at the corresponding time points using one-way analysis of variance with Bonferroni's post hoc test. Three independent experiments were performed in duplicate. Error bars, SD

VX-765 inhibited the bilirubin-induced pore formation of neuronal membranes

LDH was a major intracytoplasmic component and was released when the cell membrane ruptured. The results showed that LDH release increased as the duration of UCB stimulation lasted. The percentage of LDH release after 24 h of UCB stimulation was 37.388 ± 2.134%, which was significantly higher than that in the control group ($p < 0.001$, Fig. 3b). Meanwhile, the cells were grouped as previously described, and the LDH release rate of each group after 24 h of UCB stimulation was measured. The LDH release rate after VX-765 pretreatment was 5.867 ± 1.822%, which was significantly lower than that in the UCB group ($p < 0.001$, Fig. 3b) but higher than that in the control group ($p < 0.001$, Fig. 3b).

Then a dye staining (EtBr/EthD2) assay was performed to examine the pore formation of the neuronal membranes. Triton X-100 treatment increased the permeability of the cell membrane (Fig. 3f, j). After 24 h of UCB stimulation, the neurons of the UCB group became permeable to EtBr (Fig. 3d), while excluding EthD2 (Fig. 3h). These results revealed that membrane pore formation allowed the passage of smaller molecules, such as EtBr, but rejected larger molecules, such as EthD2. Furthermore, the percentage of EtBr-positive cells was reduced when pretreated with VX-765 from 19.148 ± 3.996% to 6.027 ± 2.298% ($p < 0.001$, Fig. 3d, e, k). However, there was no significant difference in EthD2 uptake among the control, UCB, and VX-765+UCB groups (Fig. 3g, h, i).

To analyze how caspase-1 regulated the membrane pore formation after UCB stimulation, the protein level of GSDMD was detected by western blot. The results showed that the increased expression of the cleaved GSDMD was strongly detected at 3 h ($p < 0.05$) and 6 h ($p < 0.001$) compared with the control group (0 h) (Fig. 4).

Bilirubin impacted cytokines secretion in neurons

To analyze whether the classical cytokines were secreted in neurons with UCB stimulation, first, the transcriptional levels of IL-1β and IL-18 were detected by quantitative real-time PCR. The results showed that the level of IL-1β mRNA changed in a time-dependent manner (Fig. 5a). Compared with the control group, the mRNA level of IL-1β increased significantly at 3 h ($p = 0.002$), 6 h ($p = 0.03$), and 12 h ($p < 0.001$), whereas at 24 h decreased to a level similar to that at 1 h (Fig.5a). However, UCB failed to influence the transcriptional level of IL-18 in neurons. In addition, in the cell culture supernatant, the protein levels of IL-1β, IL-18, and IL-6 were undetectable by ELISA. There was no significant difference in TNF-α secretion in the early period after UCB treatment; however, the secretion level began to increase at 24 h compared with the control group ($p < 0.001$, Fig. 5b).

VX-765 inhibited bilirubin-induced NF-κB activation

Whether other potential mechanisms of caspase-1 are involved in UCB-induced neuron damage was investigated. To analyze whether NF-κB was activated in neurons with UCB stimulation, western blot was employed to measure the protein level of NF-κB. The increased expression of NF-κB (p65) was detected 3 h after UCB treatment ($p < 0.001$), peaked at 6 h ($p < 0.001$), and then declined at 12 h (Fig. 6a). Then the NF-κB (p65) protein level at 6 h in the VX-765 + UCB group was significantly inhibited compared with that of the UCB group ($p = 0.005$, Fig. 6b) but was increased compared with that of the control group ($p < 0.001$, Fig. 6b). Subsequently, the functional activity level of NF-κB in neurons with UCB stimulation was detected by EMSA. Consistently, the results showed that NF-κB activation began to increase 1 h after the model establishment, peaked at 6 h ($p < 0.001$), and then subsequently decreased (Fig. 6c). Next, VX-765 was administered 1 h before UCB stimulation. The results revealed that the NF-κB activity level at 6 h was significantly inhibited in the VX-765+UCB group compared with the UCB group ($p = 0.015$, Fig. 6d).

DISCUSSION

Bilirubin-induced neurological dysfunction is the most severe complication of neonatal hyperbilirubinemia. Understanding how UCB causes neurotoxicity is a hot topic of current research and a prerequisite for effective prophylaxis of bilirubin encephalopathy. According to the abundant studies that were previously mentioned, the inflammatory response likely plays an important role in bilirubin neurotoxicity.

In recent years, caspase-1 has been considered to play a crucial role in regulating cellular damage and inflammation. In diseases of the central nervous system, such as Alzheimer's disease and diabetic encephalopathy,[22,23] activated caspase-1 cleaves the precursors of IL-1β and IL-18, accelerating inflammation related to cellular injury or even death. Moreover, the inhibition of its activation reduces the release of inflammatory cytokines and damage to nerve cells. In this study, the results demonstrated that UCB induced caspase-1 expression and activation in cortical neurons. Furthermore, VX-765 suppressed caspase-1 activation and increased neuronal viability. Therefore, it was speculated that the activation of caspase-1 in neurons is involved in bilirubin neurotoxicity.

Moreover, other studies have shown that caspase-1 is relevant to cell membrane rupture and is involved in producing plasma membrane pores with a functional diameter of 1.1–2.4 nm,[21,24] which is also a key characteristic of pyroptosis. In this study, the release of LDH increased as the duration of UCB stimulation lasted, whereas inhibited caspase-1 activation alleviated LDH in the

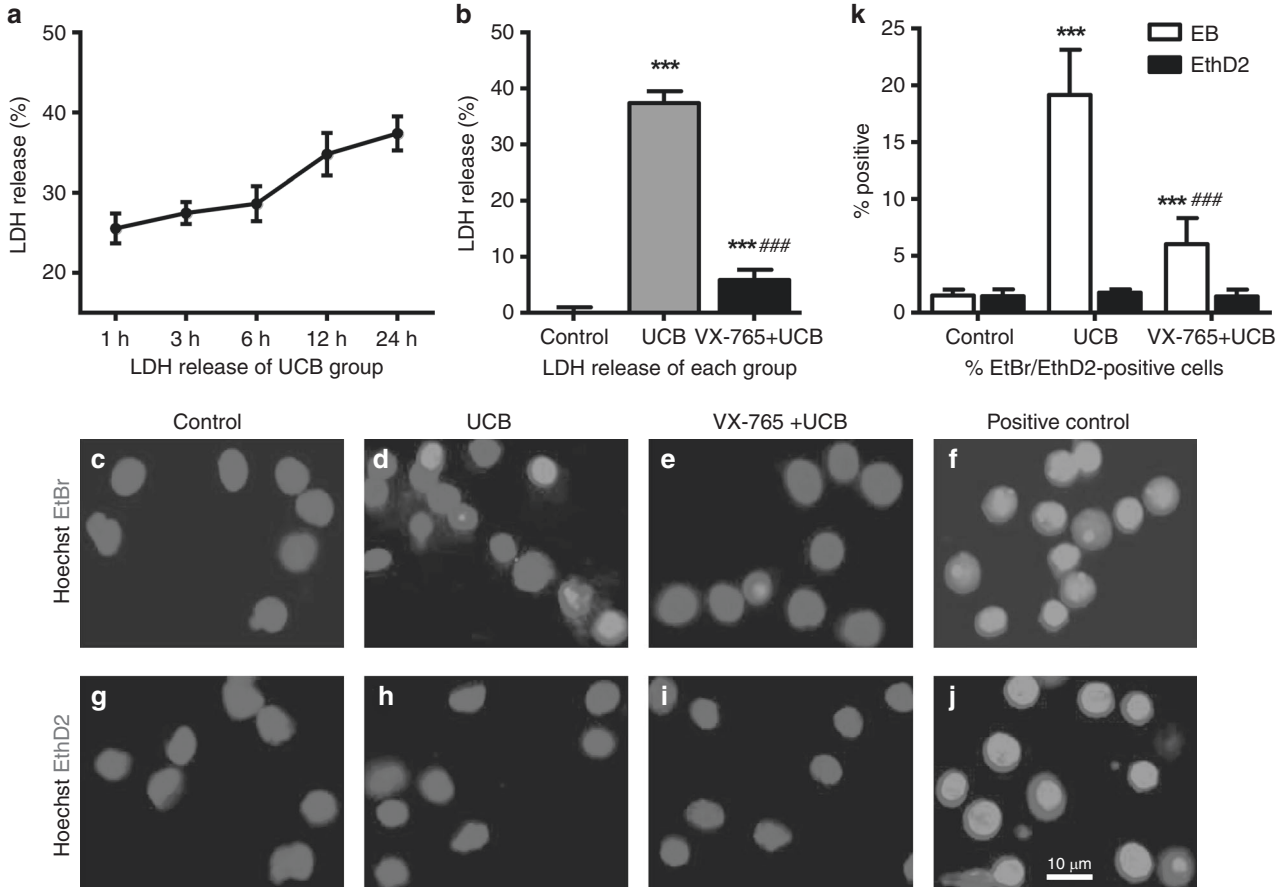

Fig. 3 Effects of VX-765 and unconjugated bilirubin (UCB) on integrity of the neuronal membrane. **a** The culture supernatant of neurons was collected for the determination of lactate dehydrogenase (LDH) release. LDH release increased as the duration of UCB stimulation lasted. **b** LDH release rate of each group at 24 h of UCB stimulation was measured. ***$p < 0.001$, versus the control group; ###$p < 0.001$, versus the UCB group using one-way analysis of variance (ANOVA) with Bonferroni's post hoc test. Three independent experiments were performed in duplicate. Error bar, SD. After the treatment, neurons adherent to glass coverslips were stained with Hoechst 33342 (blue) and EtBr (molecular weight (MW) 394 Da) or EthD2 (MW 1293 Da) (red). The adherent cells were visualized by fluorescence microscopy (×40 objective). The neurons of the control group excluded both EtBr (**c**) and EthD2 (**g**). The neurons of UCB group became permeable to ErBr (**d**) while excluding the larger EthD2 (**h**). VX-765 attenuated influx of EtBr (**e**) but had no significant effect on EthD2 uptake (**i**). The neurons treated with Triton X-100 were as a positive control, uniformly allowed influx of both EtBr (**f**) and EthD2 (**j**). A minimum of four fields from two different coverslips per sample were randomly selected to count the positive cells (red), and the results expressed as a percentage of the total nucleus population (**k**). ***$p < 0.001$, versus the control group; ###$p < 0.001$, versus the UCB group using one-way ANOVA with Bonferroni's post hoc test. The results were representative of five independent experiments. Error bars, SD

culture medium, indicating that bilirubin neurotoxicity might be related to cell membrane rupture, consistent with the previous reports.[15,19] Then cell membrane rupture was further investigated. UCB-treated neurons were stained with two red membrane-impermeant dyes, EtBr (MW 394 Da) or EthD2 (MW 1293 Da).[21] The results showed that the pore formation of the neuronal membrane with UCB stimulation allowed the uptake of EtBr without EthD2 influx. Meanwhile, VX-765 inhabited caspase-1 activation and decreased EtBr uptake, indicating that UCB induced pore formation in neuronal membranes dependent upon caspase-1 activation. Therefore, it was speculated that the UCB-induced decrease in cell viability might be related to cell membrane rupture mediated by caspase-1 activation. However, it remains unclear how caspase-1 regulates membrane pore formation after UCB stimulation. Recently, studies have discovered that GSDMD most likely induces pyroptosis, is related to membrane pore formation, and was identified as a substrate for caspase-1 and caspase-11.[25,26] In this study, the results showed that UCB induced GSDMD activation in cortical neurons. The cleavage of GSDMD by inflammatory caspases likely releases the N-terminal domain, allowing it to associate with the inner leaflet of the plasma membrane, and oligomerize to form pores that are just large enough to allow the passage of proinflammatory intracellular contents.[25,26]

In this study, the activation of caspase-1 and the formation of cell membrane pores, both of which are characteristic events of pyroptosis, simultaneously appeared in neurons treated with UCB. Pyroptosis, a "new" highly inflammatory form of programmed cell death mediated by caspase-1, has attracted widespread attention in recent years. The most significant morphological feature of pyroptosis is the formation of cell membrane pores, resulting in a loss of plasma membrane integrity. Pyroptosis allows the release of proinflammatory intracellular contents into the extracellular environment, accompanied by nuclear DNA fragmentation.[14] Therefore, it was speculated that pyroptosis might be involved in bilirubin-induced neuronal injury. Further studies are needed to prove this hypothesis.

Activated caspase-1 is required for proteolytic processing and release of the cytokines, IL-1β and IL-18. In this study, the gene expression of IL-1β increased in neurons exposed to UCB, whereas the proteins of IL-1β and IL-18 were undetectable. As we know, microglia and astrocytes are the predominant sources of

inflammatory cytokines, whereas neurons show fewer secretions of these factors. Our previous experiment reported that pyroptosis is involved in bilirubin cytotoxicity in astrocytes, causing IL-1β and IL-18 cytokine release.[15] Moreover, the reports showed that the release of TNF-α and IL-1β in cortical astrocytes with bilirubin-induced was several ten times higher than that in cortical neurons, and the inflammation reaction was more obvious in immature glial cells.[10,19] The expression of inflammatory cytokines TNF-α and IL-6 increased in UCB-treated astrocytes,[12] while in this study, the protein level of IL-6 was also undetectable, and there was no significant difference of TNF-α secretion in the early period after UCB treatment. To the increase of TNF-α secretion at 24 h, the reason probably partly owed to the reduced neuronal viability exposed to UCB. Thus neurons may react to UCB toxicity differently from microglia and astrocytes in terms of cytokine release. In addition, some experiments reported that caspase-1 contributes to the death of macrophages induced by ATP/lipopolysaccharide, independently of IL-1β and IL-18.

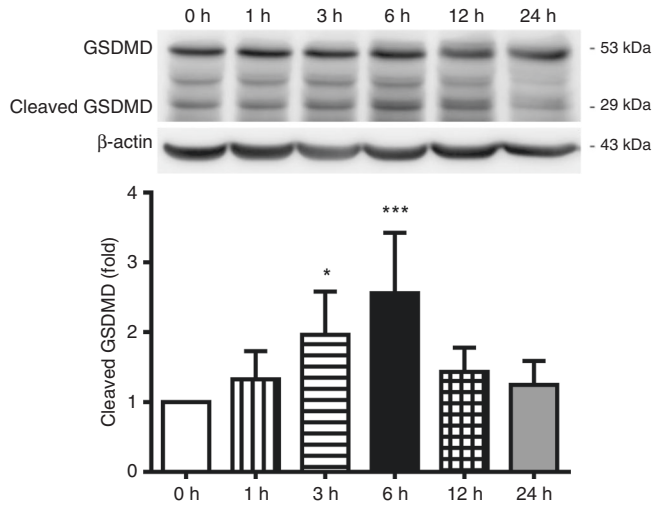

Fig. 4 Unconjugated bilirubin (UCB)-induced Gasdermin D (GSDMD) activation in cultured rat cortical neurons. The protein level of GSDMD was measured using western blot at the corresponding time points after UCB treatment. The intensity of the bands was quantitated by scanning densitometry, standardized with respect to β-actin protein, and normalized to the values of the control group (0 h). *$p < 0.05$, ***$p < 0.001$, versus the control group (0 h) using a two-tailed Student's t test with Dunnett's test. Three independent experiments were performed in duplicate. Error bars, SD

Macrophages were harvested from caspase-1, IL-18, or IL-1β knockout mice.[27] Similar results have shown that, when bone marrow-derived macrophages were infected with *S. typhimurium*, NLRC4 and caspase-1 were required for flagellin-induced bacterial clearance independently of IL-1β and IL-18. A similar phenomenon also appeared in the macrophages infected with Legionella and Burkholderia.[28] Therefore, the cleavage and release of IL-1β and IL-18 might not engage in the pathogenesis of caspase-1-mediated pyroptosis in macrophages. The effects of caspase-1 should not be identical under various stimulation and different cell types. Our results indicated that the function of caspase-1 in bilirubin neuron-toxicity was independent of IL-1β and IL-18.

Thus it is worth exploring the other potential mechanisms of caspase-1 involved in cell injury. Some reports have suggested that caspase-1 acts as an activator of NF-κB. Caspase-1 contains an N-terminal caspase recruitment domain (CARD), combined with the CARD-containing serine–threonine protein kinase RIP2 through CARD–CARD interactions. Consequently, RIP2 recruits IκB kinase complex (IKK) through a direct interaction of its intermediate domain with IKK-γ, resulting in NF-κB activation.[29,30] NF-κB, a vital transcription factor, specifically binds to the specific sites of various cellular gene promoters or enhancer sequences to promote transcription and expression.[31] The reported studies including our previous experiments suggested that the activation of NF-κB signaling appeared in neurons and glia with UCB stimulation, and double peaks of NF-κB activity had been detected.[12,32,33] It was found that the activation of NF-κB in the early period caused neuronal damage, whereas in the later period, it probably played a protective role. Therefore, we focused on the adverse effect of NF-κB on neurons in the early period, approximately 6 h after UCB stimulation. Interestingly, when pretreated with VX-765, the activation of NF-κB was suppressed, indicating that caspase-1 might regulate the activation of NF-κB. In addition, NF-κB regulates the expression of proapoptotic/antiapoptotic genes. The NF-κB-specific inhibitor upregulated the level of the antiapoptotic protein Bcl-2 but simultaneously reduced that of the proapoptotic protein Bax to restrain cell apoptosis, exhibiting a neuro-protective effect in the kernicterus model rats.[11] NF-κB also increased the expression of inflammatory cytokines, TNF-α and IL-6, in UCB-treated astrocytes and promoted the inflammatory response, aggravating cell damage.[12] Therefore, it was speculated that the activation of caspase-1 caused cell damage probably through NF-κB-mediated downstream mechanisms. Moreover, some studies have reported that the activation of NF-κB upregulates the transcription of inflammasome-related components, including inactive NLRP3, pro-IL-1β, and pro-IL-18.[34,35] Subsequently, inflammasome activation triggers the

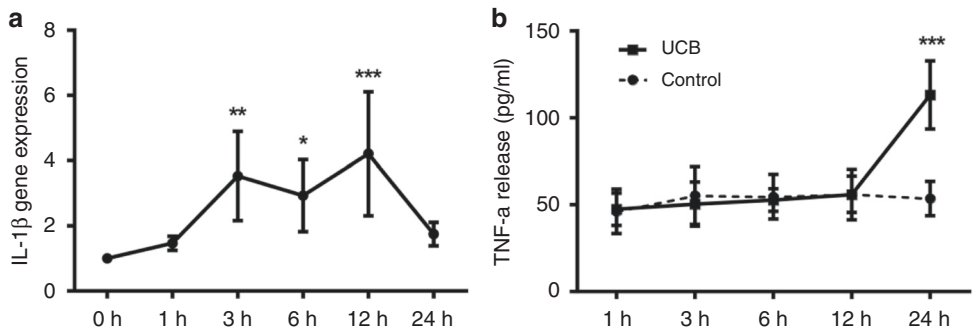

Fig. 5 Effects of unconjugated bilirubin (UCB) on cytokine secretion in cultured rat cortical neurons. **a** The mRNA level of interleukin-1β was measured by quantitative real-time reverse transcriptase-PCR at the corresponding time points after UCB treatment. *$p < 0.05$, **$p < 0.01$, ***$p < 0.001$, versus the control group (0 h) using a two-tailed Student's t test with Dunnett's test. **b** The release of tumor necrosis factor-α was measured by enzyme-linked immunosorbent assay at the corresponding time points after UCB treatment. ***$p < 0.001$, versus the control group at the corresponding time points using one-way analysis of variance with Bonferroni's post hoc test. Three independent experiments were performed in duplicate. Error bars, SD

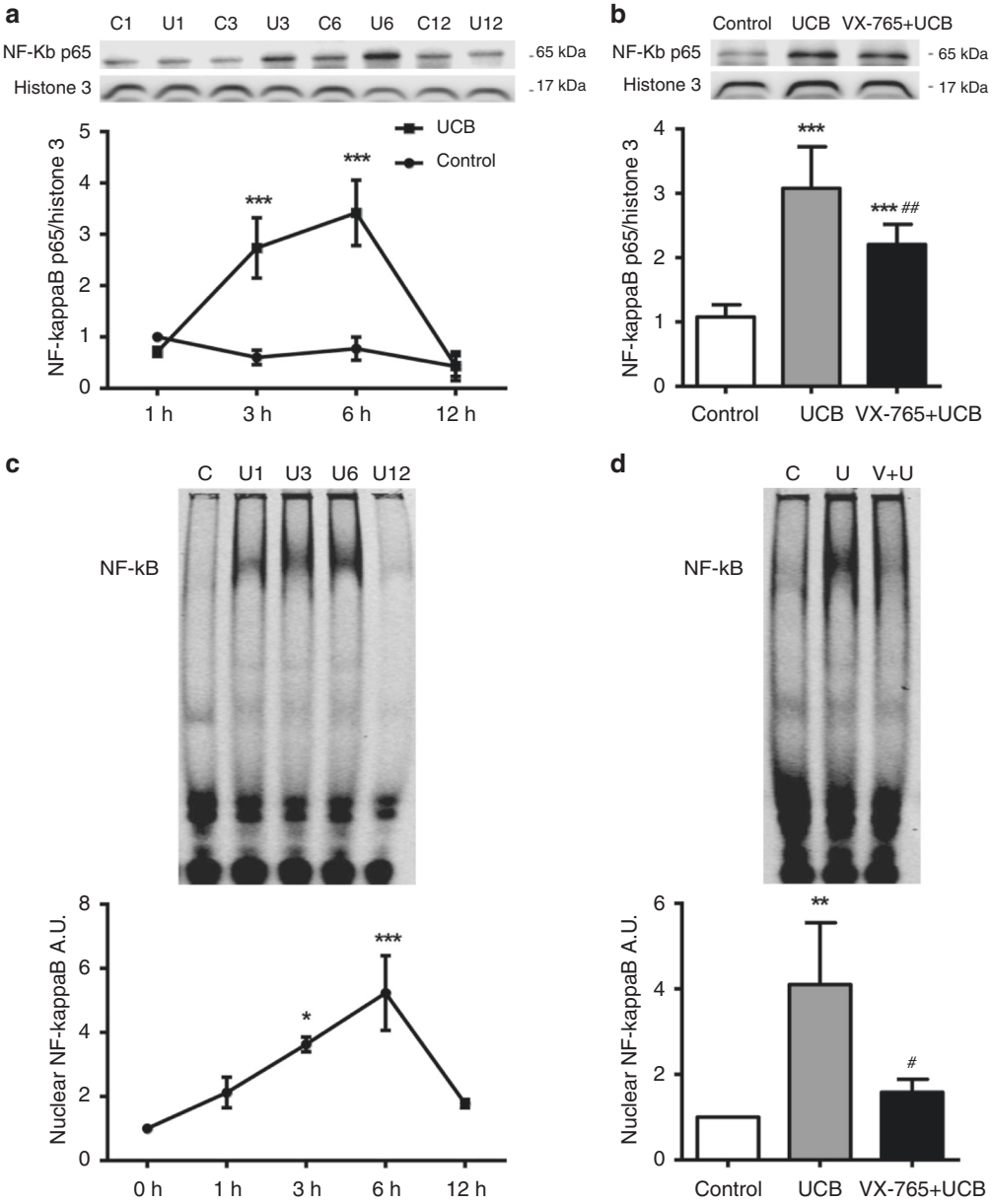

Fig. 6 Effects of VX-765 and unconjugated bilirubin (UCB) on nuclear factor-kappa B (NF)-κB activation of cultured rat cortical neurons. **a** The protein level of NF-κB was measured using western blot at the corresponding time points after UCB treatment. ***$p < 0.001$, versus the control group at the corresponding time-points using one-way analysis of variance (ANOVA) with Bonferroni's post hoc test. **b** VX-765 pretreatment inhibited NF-κB activation at 6 h after UCB stimulation. ***$p < 0.001$, versus the control group; $^{\#\#}p < 0.01$, versus the UCB group using one-way ANOVA with Bonferroni's post hoc test. The intensity of the bands was quantitated by scanning densitometry, standardized with respect to Histone 3 protein, and normalized to the values of the control group. Three independent experiments were performed in duplicate. Error bars, SD. **c** The functional activity level of NF-κB was detected by electrophoretic mobility shift assay. NF-κB activation peaked at 6 h. *$p < 0.05$, ***$p < 0.001$, versus the control group (0 h) using a two-tailed Student's *t*-test with Dunnett's test. **d** NF-κB activity level was attenuated in the VX-765 + UCB group at 6 h after UCB treatment. **$p < 0.01$, versus the control group; $^{\#}p < 0.05$, versus the UCB group using one-way ANOVA with Bonferroni's post hoc test. The intensity of the bands was quantitated by scanning densitometry and normalized to the values of the control group. Three independent experiments were performed in duplicate. Error bars, SD

transformation of pro-caspase-1 to caspase-1 and the secretion of mature IL-1β and IL-18. Therefore, complicated network regulatory mechanisms may exist in cellular defense against a variety of pathogens and stimulation, requiring further research to explore.

In conclusion, this experiment showed that caspase-1 activation was involved in neuronal damage induced by UCB. This complicated process involved the activation of caspase-1 and NF-κB, specific membrane pore formation, and programmed cell death, independently of IL-1β and IL-18.

ACKNOWLEDGEMENTS

We are grateful to Yan Zhang for excellent technical assistance during the experiments. This work was supported by the National Natural Science Foundation of China (Grant 81200459) and the Project of Basic and Frontier Research Plan of Chongqing (CSTC2018jcyjAX0284).

AUTHOR CONTRIBUTIONS

Z.H., C.H., and J.F. conceived and designed the experiments. C.H., J.F., and H.H. performed the experiments and contributed to the reagents/materials/analysis tools.

Z.H. and C.H. analyzed the data and wrote the paper. All authors read and approved the final manuscript.

ADDITIONAL INFORMATION

Competing interests: The authors declare no competing interests.

Publisher's note: Springer Nature remains neutral with regard to jurisdictional claims in published maps and institutional affiliations.

REFERENCES

1. Watchko, J. F. & Tiribelli, C. Bilirubin-induced neurologic damage-mechanisms and management approaches. *N. Engl. J. Med.* **369**, 2021–2030 (2013).
2. Reichman, N. E., Teitler, J. O., Moullin, S., Ostfeld, B. M. & Hegyi, T. Late-preterm birth and neonatal morbidities: population-level and within-family estimates. *Ann. Epidemiol.* **25**, 126–132 (2015).
3. Shapiro, S. M. Bilirubin toxicity in the developing nervous system. *Pediatr. Neurol.* **29**, 410–421 (2003).
4. Schiavon, E., Smalley, J. L., Newton, S., Greig, N. H. & Forsythe, I. D. Neuroinflammation and ER-stress are key mechanisms of acute bilirubin toxicity and hearing loss in a mouse model. *PLoS ONE* **13**, e0201022 (2018).
5. Greco, C. et al. Neonatal jaundice in low- and middle-income countries: lessons and future directions from the 2015 Don Ostrow Trieste Yellow Retreat. *Neonatology* **110**, 172–180 (2016).
6. Brito, M. A. et al. N-methyl-aspartate receptor and neuronal nitric oxide synthase activation mediate bilirubin-induced neurotoxicity. *Mol. Med.* **16**, 372–380 (2010).
7. Barateiro, A. et al. Reduced myelination and increased glia reactivity resulting from severe neonatal hyperbilirubinemia. *Mol. Pharm.* **89**, 84–93 (2016).
8. Ceulemans, A. G. et al. The dual role of the neuroinflammatory response after ischemic stroke: modulatory effects of hypothermia. *J. Neuroinflamm.* **7**, 74 (2010).
9. Joglar, B. et al. The inflammatory response in the MPTP model of Parkinson's disease is mediated by brain angiotensin: relevance to progression of the disease. *J. Neurochem.* **109**, 656–669 (2009).
10. Brites, D. The evolving landscape of neurotoxicity by unconjugated bilirubin: role of glial cells and inflammation. *Front. Pharm.* **3**, 88 (2012).
11. Li, M., Song, S., Li, S., Feng, J. & Hua, Z. The blockade of NF-κB activation by a specific inhibitory peptide has a strong neuroprotective role in a Sprague-Dawley rat kernicterus model. *J. Biol. Chem.* **290**, 30042–30052 (2015).
12. Li, S., Li, M., Zhang, Y., Feng, J. & Hua, Z. TAT-NBD exerts anti-inflammatory effect in rat cortical astrocytes by inhibiting bilirubin-induced nuclear factor-κB activation. *J. Third Mil. Med. Univ.* **37**, 2131–2136 (2015).
13. Sollberger, G., Strittmatter, G. E., Garstkiewicz, M., Sand, J. & Beer, H. D. Caspase-1: the inflammasome and beyond. *Innate Immun.* **20**, 115–125 (2014).
14. Bergsbaken, T. & Fink SI, CooksonB. T. Pyroptosis: host cell death and inflammation. *Nat. Rev. Microbiol.* **7**, 99–109 (2009).
15. Feng, J. et al. Unconjugated bilirubin induces pyroptosis in cultured rat cortical astrocytes. *J. Neuroinflamm.* **15**, 23 (2018).
16. Doitsh, G. et al. Cell death by pyroptosis drives CD4 T-cell depletion in HIV-1 infection. *Nature* **505**, 509–514 (2014).
17. Boxer, M. B. et al. A highly potent and selective caspase 1 inhibitor that utilizes a key 3-cyanopropanoic acid moiety. *ChemMedChem* **5**, 730–738 (2010).
18. Brewer, G. J., Torricelli, J. R., Evege, E. K. & Price, P. J. Optimized survival of hippocampal neurons in B27-supplemented Neurobasal, a new serum-free medium combination. *J. Neurosci. Res.* **35**, 567–576 (1993).
19. Falcão, A. S., Fernandes, A., Brito, M. A., Silva, R. F. & Brites, D. Bilirubin-induced immunostimulant effects and toxicity vary with neural cell type and maturation state. *Acta Neuropathol.* **112**, 95–105 (2006).
20. Ngai, K. C., Yeung, C. Y. & Karlberg, J. Modification of the MTT method for the study of bilirubin cytotoxicity. *Acta Paediatr. Jpn.* **40**, 313–317 (1998).
21. Fink, S. L. & Cookson, B. T. Caspase-1-dependent pore formation during pyroptosis leads to osmotic lysis of infected host macrophages. *Cell. Microbiol.* **8**, 1812–1825 (2006).
22. Heneka, M. T. et al. NLRP3 is activated in Alzheimer's disease and contributes to pathology in APP/PS1 mice. *Nature* **493**, 674–678 (2013).
23. Meng, X. F. et al. Nod-like receptor protein 1 inflammasome mediates neuron injury under high glucose. *Mol. Neurobiol.* **49**, 673–684 (2014).
24. Fink, S. L., Bergsbaken, T. & Cookson, B. T. Anthrax lethal toxin and Salmonella elicit the common cell death pathway of caspase-1-dependent pyroptosis via distinct mechanisms. *Proc. Natl Acad. Sci. USA* **105**, 4312–4317 (2008).
25. Shi, J. et al. Cleavage of GSDMD by inflammatory caspases determines pyroptotic cell death. *Nature* **526**, 660–665 (2015).
26. Kayagaki, N. et al. Caspase-11 cleaves gasdermin D for non-canonical inflammasome signalling. *Nature* **526**, 666–671 (2015).
27. Le Feuvre, R. A., Brough, D., Iwakura, Y., Takeda, K. & Rothwell, N. J. Priming of macrophages with lipopolysaccharide potentiates P2X7-mediated cell death via a caspase-1-dependent mechanism, independently of cytokine production. *J. Biol. Chem.* **277**, 3210–3218 (2002).
28. Miao, E. A. et al. Caspase-1-induced pyroptosis is an innate immune effector mechanism against intracellular bacteria. *Nat. Immunol.* **11**, 1136–1142 (2010).
29. Lamkanfi, M., Kalai, M., Saelens, X., Declercq, W. & Vandenabeele, P. Caspase-1 activates nuclear factor of the kappa-enhancer in B cells independently of its enzymatic activity. *J. Biol. Chem.* **279**, 24785–24793 (2004).
30. Moon, P. D. & Kim, H. M. Thymic stromal lymphopoietin is expressed and produced by caspase-1/NF-κB pathway in mast cells. *Cytokine* **54**, 239–243 (2011).
31. Mincheva-Tasheva, S. & Soler, R. M. NF-κB signaling pathways: role in nervous system physiology and pathology. *Neuroscientist* **19**, 175–194 (2013).
32. Song, S., Zhu, Y., Dang, S., Wang, S. & Hua, Z. Role of nuclear factor-κB activation in bilirubin-induced rat hippocampal neuronal apoptosis and the effect of TAT-NBD intervention. *J. South Med. Univ.* **33**, 172–176 (2013).
33. Silva, S. L. et al. Features of bilirubin-induced reactive microglia: from phagocytosis to inflammation. *Neurobiol. Dis.* **40**, 663–675 (2010).
34. Bauernfeind, F. G. et al. Cutting edge: NF-kappaB activating pattern recognition and cytokine receptors license NLRP3 inflammasome activation by regulating NLRP3 expression. *J. Immunol.* **183**, 787–791 (2009).
35. Franchi, L., Muñoz-planillo, R. & Núñez, G. Sensing and reacting to microbes through the inflammasomes. *Nat. Immunol.* **13**, 325–332 (2012).